Available online at www.sciencedirect.com
ScienceDirect
Ceramics International 36 (2010) 2181–2188
CERAMICS INTERNATIONAL
www.elsevier.com/locate/ceramint

Toughening of SiC matrix with *in-situ* created TiB_2 particles

Dusan Bucevac [a,b], Snezana Boskovic [b], Branko Matovic [b], Vladimir Krstic [a,*]

[a] *Department of Mechanical and Materials Engineering, Queen's University, Kingston, Ontario K7L 3N6, Canada*
[b] *Institute of Nuclear Sciences Vinca, P.O. Box 522, Belgrade 11001, Serbia*

Received 5 March 2010; received in revised form 7 April 2010; accepted 7 May 2010
Available online 25 June 2010

Abstract

SiC–TiB_2 composites with up to 50 vol% TiB_2 were fabricated by *in-situ* reaction between TiO_2, B_4C and C. The densification of the uniaxially pressed samples was done using pressureless sintering in the presence of sintering aids consisting of Al_2O_3 and Y_2O_3. The influence of the volume fraction of TiB_2 and sintering temperature on density and fracture toughness was examined. It was found that fracture toughness is strongly affected by the volume fraction of TiB_2. The presence of TiB_2 particles suppresses the grain growth of SiC and facilitates different toughening mechanisms to operate which, in turn, increases fracture toughness of the composite. The highest value for fracture toughness of 5.7 MPa $m^{1/2}$ was measured in samples with 30 vol% TiB_2 sintered at 1940 °C.

Keywords: A. Sintering; B. Composites; C. Toughness and toughening; D. SiC

1. Introduction

Combination of properties such as low specific gravity, high strength and hardness, good oxidation resistance, high thermal conductivity and low thermal expansion coefficient makes SiC attractive material for various applications at both room and elevated temperatures. However, its relatively low fracture toughness limits the use of SiC to applications where reliability is not the primary prerequisite. One of the methods of improving fracture response of SiC is the development of microstructure consisting of elongated grains in a matrix of equiaxed or slightly elongated grains [1,2]. The elongated grains can act as a reinforcing phase that promotes crack bridging [3,4] and crack deflection mechanisms [5], resulting in improved fracture toughness. The contribution of these mechanisms to toughening strongly depends on the morphology of elongated grains. Although the presence of elongated grains is normally highly beneficial in increasing fracture toughness, in some cases, their presence can cause a decrease in strength [6,7].

The use of TiB_2 particles uniformly distributed in SiC matrix was found to be a convenient approach to both restricting the growth of large elongated SiC grains and increasing the fracture toughness of the composite [8]. Higher linear thermal expansion coefficient of TiB_2 (8.65×10^{-6} °C^{-1}) compared to that of SiC (4.16×10^{-6} °C^{-1}) is expected to create compressive residual thermoelastic stress in SiC matrix near the TiB_2–SiC interface [9]. The results of the interaction between the tensile stress field at the crack tip and the compressive stress around the TiB_2 particles are the reduction of stress intensification factor and an increase in fracture toughness of the composite [10,11]. This toughening mechanism is usually called toughening due to residual thermoelastic stress in two-phases system.

In the past, most of the work in this area was centered on blending the SiC with TiB_2 powder. Due to relatively coarse and often inactive commercially available TiB_2 powder, the mixture could rarely be sintered to high density using pressureless sintering and hot pressing was the only viable technique capable of providing high density [12,13]. The objective in this paper is to replace the hot pressing with a less expensive pressureless sintering technique using *in-situ* created TiB_2 particles. Instead of mixing SiC with the commercially available TiB_2 powder, the composite consisting of SiC matrix and TiB_2 particles was fabricated by mixing TiO_2 with B_4C, carbon and SiC and densifying the composite at a selected temperature. Before reaching the sintering temperature, the

* Corresponding author. Tel.: +1 613 533 2760; fax: +1 613 533 6610.
E-mail address: krsticv@queensu.ca (V. Krstic).

0272-8842/$36.00.
doi:10.1016/j.ceramint.2010.06.001

affinity of B for Ti leads to the formation of TiB_2 according to the following reaction [14]:

$$2TiO_2 + B_4C + 3C \rightarrow 2TiB_2 + 4CO\uparrow \quad (1)$$

The *in-situ* formed TiB_2 particles possess high surface area and driving force for sintering sufficiently high to allow densification of the composites to densities exceeding 98% of the theoretical density without the application of external pressure. The substitution of SiC particles with TiB_2 particles also helps to suppress the weight loss created due to the reaction between SiC and sintering aids such as Al_2O_3 and Y_2O_3, used in this system to create liquid phase and promote densification [15]. The present paper presents the results on microstructure development and fracture toughness in SiC–TiB_2 composites containing up to 30 vol% *in-situ* formed TiB_2 particles.

2. Experimental procedure

Commercially available β-SiC with an average particle size of 0.7 μm (Functional Materials Manufacturing, Canada), Al_2O_3 powder (A-16 SG, Alcoa, USA), high purity Y_2O_3 powder (Alpha Aesar, USA), sub-micrometer TiO_2 powder (anastase type, Fuji-Titan, Japan), sub-micrometer B_4C powder (Electro Abrasive, USA)) and high surface area graphite powder (Aldrich Chemical Company, USA) were used as raw materials. The amount of TiO_2, B_4C and C was adjusted so as to yield volume fractions of TiB_2 particles ranging from 6 to 50 vol%. Al_2O_3 and Y_2O_3 were used as sintering aids at the level of 4.3 and 5.7 wt%, respectively. The starting powders and binder (5 wt% polyethylene-glycol) were mixed by ball milling in a plastic jar using ZrO_2 as a milling media. Methanol was used as a liquid vehicle and milling time was 12 h. After drying and screening, the powder batches were compacted by cold uniaxial pressing at a pressure of 50 MPa into rectangular shape green compacts with approximate dimensions 35 mm × 16 mm × 8 mm. In order to increase the green density and make it uniform, all green compacts were isostatically pressed under pressure of 250 MPa. The sintering was done by heating the samples to 1450 °C under vacuum and holding at that temperature for 1 h, before reaching the sintering temperature, in order to allow the reaction between TiO_2, B_4C and C to take place and fully convert TiO_2 to TiB_2. After 1 h, argon was introduced and the samples were heated up to the final sintering temperature. Sintering temperature was varied from 1820 to 1970 °C with an increment of 30 °C. The samples were held at sintering temperature for 1 h before cooling down. Sintered samples were machined into rectangular bars with approximate dimensions 3 mm × 4 mm × ~27 mm.

The density of the samples was measured using Archimedes' method. The relative density was calculated based on the theoretical density (TD) which was calculated using a rule of mixture. The crystalline phases were determined by XRD method. Fracture toughness was measured by indentation method using Vicker's indenter. The following equation proposed by Anstis was used for fracture toughness calculation [16]:

$$K_{IC} = 0.016\left(\frac{E}{H}\right)^{0.5}\frac{P}{C^{1.5}} \quad (2)$$

where E is the Young's modulus, H is the Vicker's hardness, P is the indentation load (20 kg) and C is the half-length of radial crack. The Young's modulus of SiC–TiB_2 composite was calculated according to a rule of mixture.

Fracture toughness of one series of samples was measured by the four-point notch method in order to compare the results with the indentation method. A sharp crack at the notch's tip, approximately 30–60 μm in length, was introduced by a laser. The fracture toughness was calculated using the equation [17]:

$$K_{IC} = \frac{P_{\max}}{W\sqrt{H}}\frac{S-s}{H}\frac{3\Gamma\sqrt{\alpha}}{2(1-\alpha)^{3/2}} \quad (3)$$

where $P_{\max}$ is the maximum load, W is the width and H is the height of the bar, S and s are the outer span (24 mm) and the inner span (13 mm) of the jig, respectively, $\alpha = a/H$ where a is the total length of the notch and the sharp crack at the notch's tip, and $\Gamma = 1.9887 - 1.326\alpha - (((3.49 - 0.68\alpha + 1.35\alpha^2)\alpha(1-\alpha))/(1+\alpha)^2)$. Six bars were tested for each composition and an average value was chosen.

The microstructures of polished, fractured and etched surfaces were observed by optical and scanning electron microscopy (SEM). The length and the width of SiC grains were measured manually on etched surfaces using Image-Pro Plus software. The polished surfaces were electrochemically etched in KOH solution.

3. Results and discussion

3.1. Densification

The effect of sintering temperature and volume fraction of TiB_2 on density of samples containing up to 30 vol% TiB_2 is presented in Fig. 1. The figure shows that densities of over 97% TD are achieved in the samples containing TiB_2 in the temperature range between 1850 and 1940 °C. The density of sintered samples increases with sintering temperature reaching a maximum at a certain temperature, which depends on the volume fraction of TiB_2 particles. Samples containing 0 vol% (monolithic SiC) and 6 vol% TiB_2 have a maximum in density at ~1850 °C. Somewhat lower density of the samples containing TiB_2 compared to that of a monolithic SiC is caused by the weight loss through CO evolution during $TiO_2 \rightarrow TiB_2$ conversion (Eq. (1)). The result of the conversion reaction is the increase in porosity of the compacts in proportion to the level of TiO_2 added to the SiC. As the level of TiO_2 is increased the higher level of porosity raises the temperature required for sintering. As Fig. 1 shows, a maximum in density of samples with 12–30 vol% TiB_2 is measured at ~1940 °C. At this temperature, the density of samples containing TiB_2 is more than 1% higher than that of monolithic SiC. There are two reasons for higher density of samples containing TiB_2. The first reason is the increased driving force

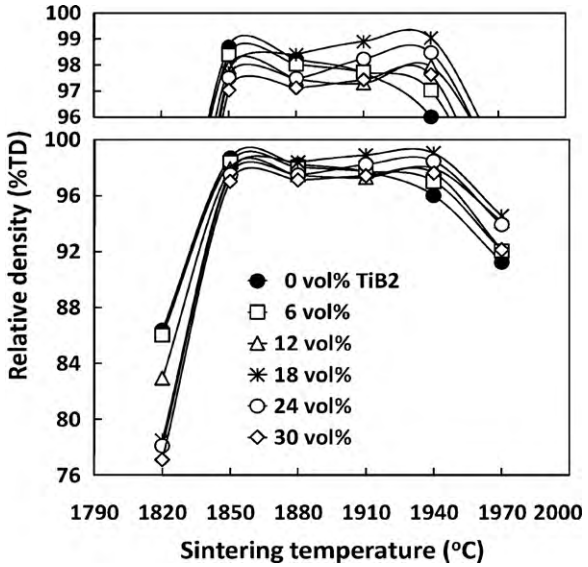

Fig. 1. Density of samples with different volume fractions of TiB_2 as a function of sintering temperature.

for sintering due to the presence of very fine and active *in-situ* formed TiB_2 particles. The second reason is the suppression of the reaction between SiC and Al_2O_3 [15] due to the replacement of SiC particles by TiB_2 particles. The reaction results in the formation of highly volatile Al_2O phase which retards densification. As Fig. 1 indicates, when sintering temperature is increased above ~1940 °C the reaction between SiC and Al_2O_3 (sintering aid) becomes intensive causing the decrease in density of all compositions. The intensity of the reaction between SiC and Al_2O_3 is best illustrated through the change in weight loss with sintering temperature as presented in Fig. 2. In order to separate the weight loss due to the reaction between SiC and Al_2O_3 and the weight loss due to *in-situ* formation of TiB_2, the amount of CO gas created during the TiB_2 formation was calculated according to the stoichiometry of Eq. (1) and subtracted from the total, measured weight loss. As Fig. 2 shows, the relatively small weight loss due to the reaction between SiC and Al_2O_3 is measured in all samples at

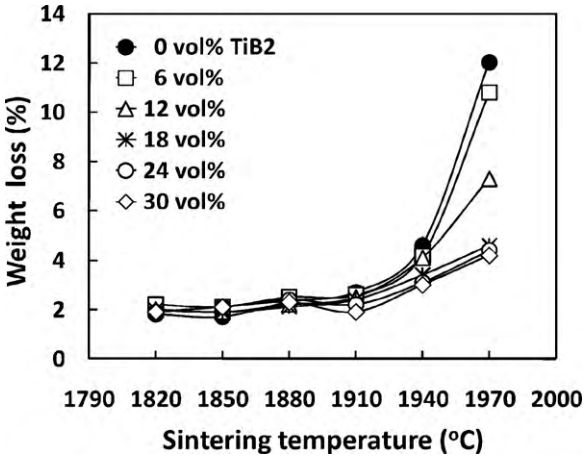

Fig. 2. Weight loss in samples with different volume fractions of TiB_2 as a function of sintering temperature.

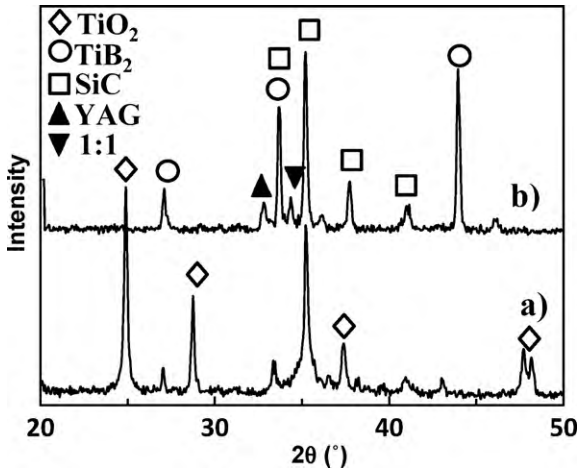

Fig. 3. X-ray patterns of samples with 24 vol% TiB_2 a) before sintering (~27.5 wt% TiO_2 prior to the $TiO_2 \rightarrow TiB_2$ conversion) and b) after sintering at 1940 °C.

temperatures bellow approximately 1940 °C. Once the sintering temperature exceeds 1940 °C, rapid increase in weight loss is observed with the highest loss measured in monolithic SiC. The reason for smaller weight loss in the samples containing TiB_2 particles compared to monolithic SiC is the reduced contact points between SiC and Al_2O_3 and the increased contact area between SiC and TiB_2.

3.2. Phase composition

The XRD analysis performed on the samples before and after sintering at 1940 °C is given in Fig. 3 for composite with 24 vol% TiB_2. Fig. 3 shows complete conversion of TiO_2 to TiB_2 without any detectable amount of unconverted oxide or traces of side products which could be created during the conversion reaction. Besides SiC and TiB_2, two alumina–yttria crystalline phases are observed. The first phase is the yttria alumina garnet (YAG) with formula $3Y_2O_3{\cdot}5Al_2O_3$whereas the second phase is known as 1:1 phase with formula $Y_2O_3{\cdot}Al_2O_3$ [18]. Both phases are located between SiC and TiB_2 grains and considered to be the result of crystallization of the liquid phase during cooling from the sintering temperature.

3.3. Fracture toughness

The change in fracture toughness with sintering temperature for samples with different volume fractions of TiB_2 particles is shown in Fig. 4. The fracture toughness of samples sintered at temperatures below 1850 °C as well as samples sintered at temperatures above 1940 °C will not be discussed since the densities were well below 95% TD, which is considered to be too low for structural application. The small increase in fracture toughness with increase in sintering temperature, observed in Fig. 4, is believed to be mainly due to the elongation of SiC matrix grains and their enhanced contribution to toughening by crack deflection and crack bridging [1,2]. Furthermore, the improved fracture toughness of samples with 24 vol% TiB_2

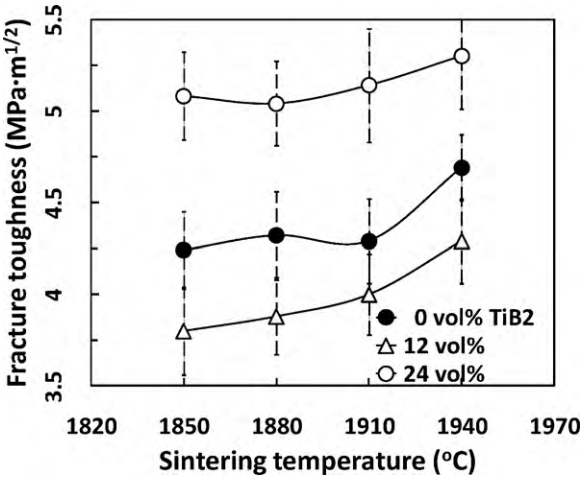

Fig. 4. Effect of sintering temperature on fracture toughness of samples with different volume fractions of TiB_2.

compared to that of monolithic SiC is considered to be the result of relaxation of the tensile stress at the crack tip due to the interaction with the compressive stress outside of TiB_2 particles. As mentioned, the tangential compressive stress in the surrounding SiC matrix is created due to larger shrinkage of TiB_2 particles compared to that of SiC matrix on cooling to room temperature [10]. Besides stress relaxation, the TiB_2 particles are expected to deflect the crack, also resulting in a reduction of the stress at the crack tip and consequent increase in fracture toughness of the composite. However, the lower fracture toughness of samples containing 12 vol% TiB_2 than that of monolithic SiC, is believed to be the result of suppression of elongation of SiC grains by the presence of TiB_2 which, in turn, decreases fracture toughness of the SiC matrix and therefore the overall fracture toughness of the composite. The volume fraction of TiB_2 appears to play the key role in determining which of the above-mentioned effects of TiB_2 on fracture toughness is dominant and whether fracture toughness of the composite is lower or higher than that of a monolithic SiC. To further examine the effect of volume fraction of TiB_2 on microstructure of the SiC matrix and fracture toughness of the composite, the samples sintered at 1940 °C are selected. The temperature of 1940 °C is chosen since it gives the samples with the highest fracture toughness and provides the optimum density for the samples containing larger volume fractions of TiB_2 (12–30 vol%) (Fig. 1).

3.4. Microstructure and fracture toughness of samples sintered at 1940 °C

Fig. 5 shows the microstructure of etched surfaces of samples with different volume fractions of TiB_2. It is clear from Fig. 5 that the increase in volume fraction of TiB_2 (white phase) decreases the length of SiC grains (grey phase) as well as their aspect ratio which is defined as the ratio between the length and the width of the grains. For example, the length of the SiC grains in monolithic SiC is well above 35 μm (Fig. 5(a)), whereas no grain longer than 10 μm is observed in the sample with 30 vol% TiB_2 (Fig. 5(d)). It is also observed from Fig. 5 that the volume fraction of equiaxed SiC grains increases as the volume fraction of TiB_2 increases. Knowing that the equiaxed

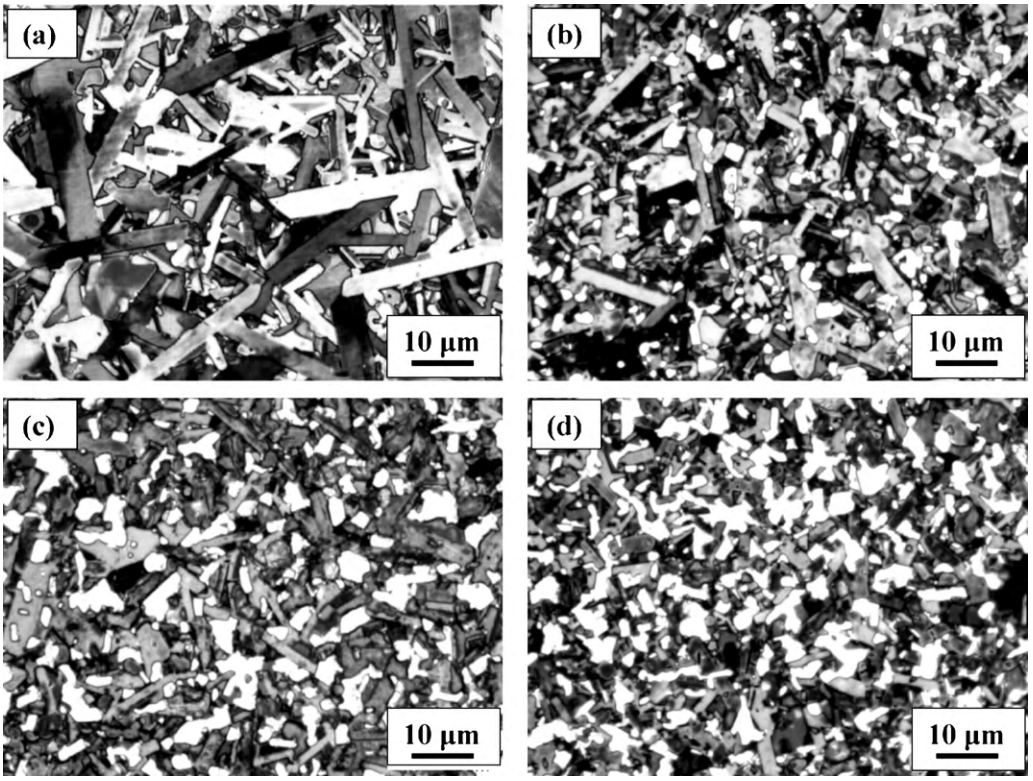

Fig. 5. Optical micrographs of etched surfaces of samples sintered at 1940 °C with (a) 0 vol%, (b) 12 vol%, (c) 24 vol%, and (d) 30 vol% TiB_2 (white areas).

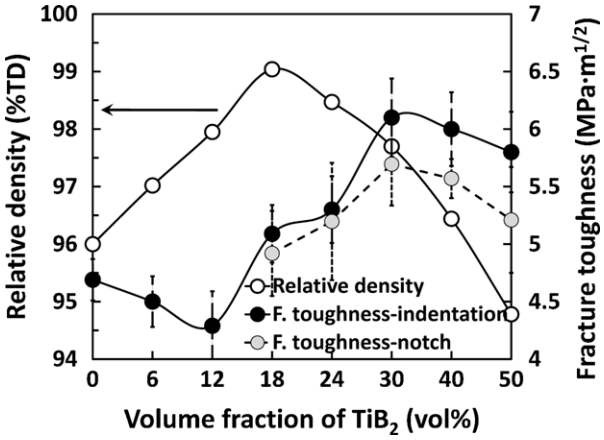

Fig. 6. Fracture toughness and density of samples sintered at 1940 °C as a function of volume fraction of TiB_2. Fracture toughness was measured by indentation as well as four-point notch method.

SiC grains have small contribution to crack deflection and crack bridging [3–5], the SiC matrix in samples containing TiB_2 is expected to have lower fracture toughness than the monolithic SiC sintered at the same temperature.

The relation between density, volume fraction of TiB_2 and fracture toughness (measured by indentation) for samples sintered at 1940 °C is presented in Fig. 6. At lower volume fractions of TiB_2 (6–12 vol%), the presence of TiB_2 particles inhibits the growth of SiC grains leading to a decrease in fracture toughness of the SiC matrix and thus to a decrease in fracture toughness of the composite. When the volume fraction of TiB_2 exceeds ~12 vol% the presence of TiB_2 particles increases the frequency of interaction of crack tip with the particles (Fig. 7(b) and (c)) the effect of which is the increase in fracture toughness (Fig. 6). Clearly, this interaction dominates toughening process and causes a continuous increase in fracture toughness of the composite. Above approximately 15 vol% TiB_2, the level of fracture toughness of the composites exceeds the level of fracture toughness of the monolithic SiC. The highest fracture toughness of 6.1 MPa $m^{1/2}$ was obtained in the samples containing ~30 vol% TiB_2. It is interesting to note that the fracture toughness continues to increase for all compositions from 12 to 30 vol% TiB_2 in spite of the fact that the density of the samples with above ~18 vol% starts to decrease. Only when the volume fraction of TiB_2 exceeds ~30 vol% the fracture toughness starts to decrease due to a sharp decrease in density. As Fig. 6 shows, the density increases with an increase in volume fraction of TiB_2 reaching a maximum in samples with 18 vol% TiB_2. The reason for a decrease in the density of samples with the volume fractions of TiB_2 above ~18 vol% is the increased green porosity created after *in-situ* formation of TiB_2. Despite the creation of additional porosity, the samples with 30 vol% TiB_2 have fairly high density, i.e., above 97.5% TD.

It is considered appropriate at this point to discuss the reliability of the indentation technique used for fracture toughness measurements. The rationale for using the indentation method is based on the fact that it is a simple and fast method requiring an inexpensive hardness measurement

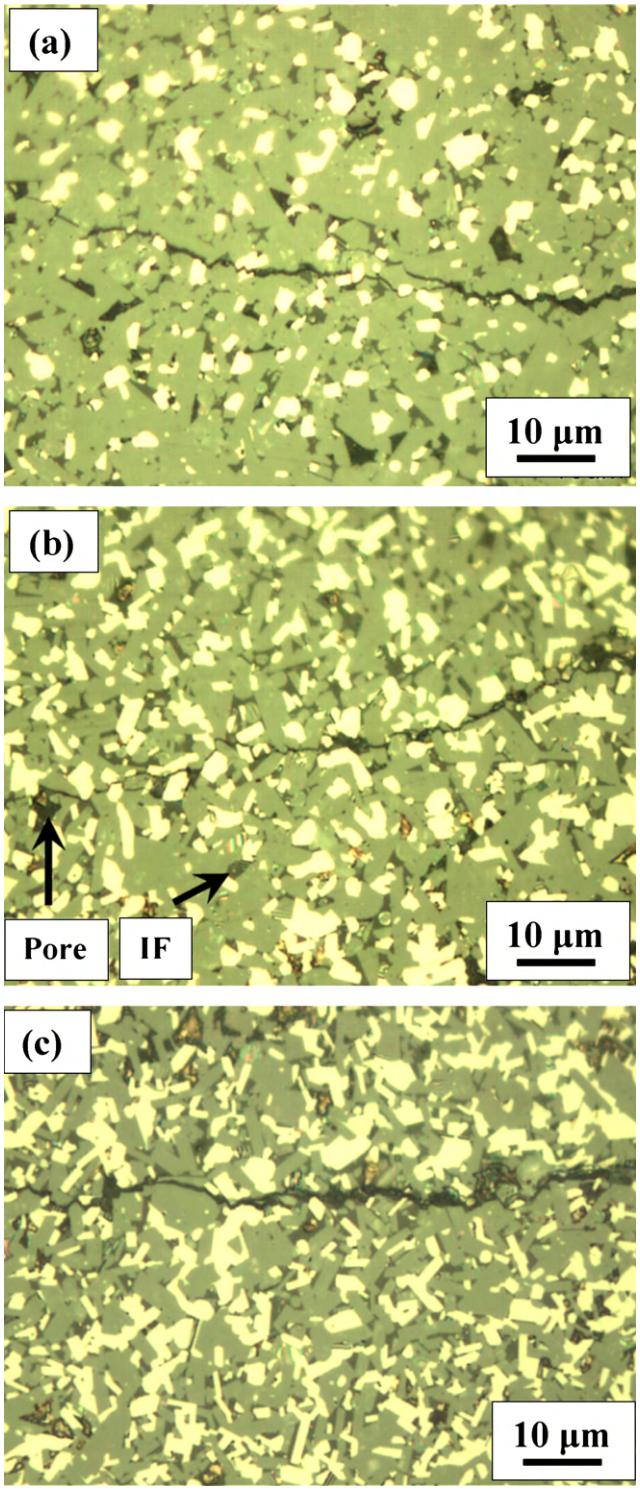

Fig. 7. Optical micrographs of crack propagation in samples sintered at 1940 °C with (a) 12 vol%, (b) 24 vol%, and (c) 30 vol% TiB_2 (bright areas). Black areas represent porosity and grain pull-out that occurs during polishing. Note that the intergranular phase (IF) is brighter than porosity.

apparatus. Problems arise when measurements are done on samples with high levels of porosity such as the case with samples containing more than 24 vol% TiB_2. The collapse of the porosity absorbs some of the dilatation due to the indentation which results in shorter cracks emanating from

an indent. For this reason the fracture toughness of samples containing 18–50 vol% TiB_2 was also measured by the notch method and given in Fig. 6. The small difference in fracture toughness between the indentation and four-point notch method for samples containing 18 and 24 vol% TiB_2, suggests that the high density of these samples (>98% TD) allows an accurate measurement of fracture toughness by indentation method. Although the difference in fracture toughness is larger in samples with lower density (>24 vol% TiB_2) the notch method proves that samples with 30 vol% TiB_2 have the highest fracture toughness. Now, one can argue that the fracture toughness of samples with 0 vol% TiB_2, which have density about 96% TD, is also overestimated and could be even lower than that of samples with 12 vol% TiB_2 (Fig. 6). This argument does not support the previously inferred conclusion that the presence of up to 12 vol% TiB_2 suppresses the elongation of SiC matrix grains and decreases the overall fracture toughness of the composite. However, it is important to stress that the further support to the inferred conclusion was found from Fig. 4, which showed that the lower fracture toughness of samples with 12 vol% TiB_2 than that of monolithic SiC was also measured in samples with densities above 98% TD such as those sintered at 1910 °C. The indentation measurements in these samples were not obscured by porosity and the change in fracture toughness was predominantly caused by the change in microstructure.

Fig. 8 shows the fracture surfaces of samples with 0 and 30 vol% TiB_2 sintered at 1940 °C. As shown, very long and thick SiC grains in samples without TiB_2 (Fig. 8(a)) as well as equiaxed grains in samples with 30 vol% TiB_2 (Fig. 8(b)) appear not to undergo pull-out in any substantial degree. As Fig. 8(a) indicates, the very long SiC grains in monolithic SiC are prone to fracture transgranularly, whereas the considerable level of intergranular crack propagation is observed in the samples with 30 vol% TiB_2 (Fig. 8(b)).

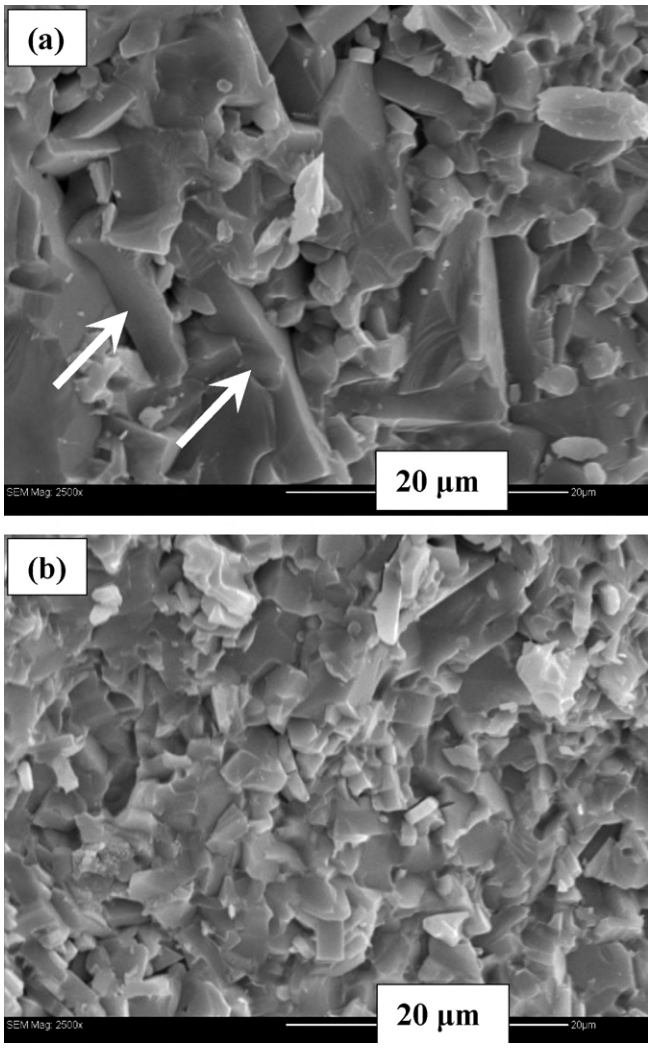

Fig. 8. SEM micrographs of fracture surfaces of samples sintered at 1940 °C (a) with 0 vol% and (b) with 30 vol% TiB_2. The arrows indicate transgranular fracture of long SiC plates.

3.5. Theoretical analysis

In this section an effort is made to quantify the effect of the volume fraction and morphology of the elongated SiC grains on fracture toughness of the SiC matrix. The analysis is centered on crack deflection as the dominant toughening mechanism operating in the SiC matrix. If it is assumed that the elongated SiC grains are approximately disc-shaped, the contribution of these grains to toughening by crack deflection can be expressed by the following equation [5]:

$$K_m = K_{eq}\left(1 + 0.28V\frac{l}{d}\right) \quad (4)$$

where K_m is the fracture toughness of SiC with elongated grains, i.e., the fracture toughness of SiC matrix, K_{eq} is the fracture toughness of SiC with equiaxed grains, V is the volume fraction of the elongated grains in SiC matrix, and l and d are the length and width of the elongated SiC grains, respectively. Eq. (4) is used to predict/calculate fracture toughness of the SiC matrix based on the volume fraction (V) and aspect ratio (l/d) of the elongated SiC grains. In this calculation, the contribution of TiB_2 particles to toughness by crack–particle interaction is excluded entirely. In order to perform this calculation, it is necessary to determine the values for volume fraction, length and width of the elongated grains in the SiC matrix. This was done on etched surfaces of the samples containing 0, 12, 24 and 30 vol% TiB_2. Based on the literature value for fracture toughness of the equiaxed SiC [6,9,12], K_{eq}, of 3.3 MPa $m^{1/2}$ and the measured values for volume fraction, length and width of the elongated SiC grains, the fracture toughness of SiC without TiB_2 particles, i.e., the fracture toughness of the SiC matrix, K_m, is calculated (using Eq. (4)) and compared with the measured fracture toughness of the samples containing 0, 12, 24 and 30 vol% TiB_2 (Table 1). As expected, the fracture toughness of SiC matrix decreases continuously with the volume fraction of TiB_2 due to a decrease in aspect ratio and volume fraction of elongated SiC grains. The reason for the higher calculated than the measured fracture toughness of monolithic SiC (0 vol% TiB_2) is the overestimated contribution of very long SiC grains to toughening by crack deflection. The support to this is found

Table 1
Calculated fracture toughness (via Eq. (4)) of SiC matrix in samples sintered at 1940 °C.

Volume fraction of TiB_2 (vol%)	Volume fraction of elongated SiC grains V (vol%)	Elongated SiC grains			Calculated fracture toughness of SiC matrix K_m (MPa $m^{1/2}$)	Measured fracture toughness of the composite, indentation (MPa $m^{1/2}$)
		Average length l (μm)	Average width d (μm)	Aspect ratio (l/d)		
0	47 ± 2	17.1 ± 6.6	2.7 ± 0.7	6.3	6.1	4.7 ± 0.4
12	33 ± 2	9.9 ± 3.2	2.2 ± 0.3	4.5	4.7	4.3 ± 0.3
24	27 ± 2	8.1 ± 2.1	2.1 ± 0.3	3.9	4.3	5.3 ± 0.3
30	20 ± 1	5.9 ± 1.6	1.8 ± 0.3	3.3	3.9	5.7 ± 0.4[a]

[a] Measured by the notch method.

from the observation made on fracture surface (Fig. 8(a)) which indicates that, despite the high aspect ratio of very long SiC grains, most of them fracture transgranularly (with low contribution to toughening) rather then intergranularly. Based on this, one can argue that not all elongated SiC grains contribute to toughening but only a fraction of them. For example, if it is assumed that only 50% of elongated SiC grains in monolithic SiC contribute to toughening by crack deflection, the calculated value for K_m becomes almost identical to the measured value. As the volume fraction of TiB_2 particles increases, their contribution to overall toughening of the composite increases, suggesting that the crack–particle interaction mechanism of toughening starts to dominate the overall toughness. By comparing the predicted value for fracture toughness of SiC matrix and the measured value for fracture toughness of the composite with 30 vol% TiB_2 (Table 1) one finds that ~32% of the total measured toughness comes from the TiB_2 particles and ~68% from the SiC matrix.

Earlier it has been suggested that the presence of TiB_2 particles in the SiC matrix contributes to the overall toughness of the composite through two different mechanisms; crack deflection and crack tip–residual stress field interaction. It would be now of interest to estimate the contribution of each toughening mechanism to the overall toughness of the composite. The contribution of crack deflection due to the presence of equiaxed TiB_2 particles to toughening can be estimated using the following equation [5]:

$$K_{IC}^{def} = (1 + 0.87V_{TiB_2})K_m \quad (5)$$

where K_{IC}^{def} is the fracture toughness of the composite due to deflection by TiB_2 particles, V_{TiB_2} is the volume fraction of TiB_2 particles and K_m is the fracture toughness of SiC matrix. Substituting the values: $V_{TiB_2} = 0.30$ and $K_m = 3.9$ MPa $m^{1/2}$ (Table 1) into Eq. (5), the fracture toughness of the composites with 30 vol% TiB_2 is calculated to be 4.9 MPa $m^{1/2}$. This value indicates that the contribution of crack deflection due to the presence of TiB_2 particles to toughening is ~1 MPa $m^{1/2}$. The difference between the measured fracture toughness of the composite (5.7 MPa $m^{1/2}$) and the calculated fracture toughness due to deflection by TiB_2 particles (K_{IC}^{def}) suggests that the contribution of crack tip–residual stress field interaction to toughening is ~0.8 MPa $m^{1/2}$. It appears that the contributions of two toughening mechanisms activated by the presence of TiB_2 particles are almost the same in composites with 30 vol% TiB_2.

4. Conclusions

It was possible to sinter SiC ceramics in the presence of 30 vol% of *in-situ* formed TiB_2 particles to densities of over 97% TD without the application of external pressure. High density was achieved with the help of Al_2O_3 and Y_2O_3 sintering aids. The presence of *in-situ* formed TiB_2 particles with very small particle size and high activity served to enhance the driving force for sintering. In addition to densification, the presence of TiB_2 in SiC matrix had two important effects on fracture toughness of the composite. The first effect comes from the suppression of growth of SiC grains and consequent decrease in fracture toughness of the SiC matrix. The second effect comes from the activation of additional toughening mechanisms such as crack deflection and toughening due to residual thermoelastic stress. Which effect dominates the toughening depends on the volume fraction of TiB_2 particles. The presence of more than ~15 vol% TiB_2 particles increases the fracture toughness of the composite above the fracture toughness of monolithic SiC. The highest fracture toughness of 5.7 MPa $m^{1/2}$ was measured in samples containing 30 vol% TiB_2. The high fracture toughness of these samples was found to be the result of high contribution of toughening mechanisms activated by the presence of TiB_2 particles.

References

[1] S.G. Lee, Y.W. Kim, M.J. Mitomo, Relationship between microstructure and fracture toughness of toughened silicon carbide ceramics, J. Am. Ceram. Soc. 84 (6) (2001) 1347–1353.
[2] H. Xu, T. Bhatia, S.A. Deshpande, N.P. Padture, A.L. Ortiz, F.L. Cumbrera, Microstructural evolution in liquid-phase-sintered SiC: Part I. Effect of starting powder, J. Am. Ceram. Soc. 84 (7) (2001) 1578–1584.
[3] B. Budiansky, J. Amazigo, Toughening by aligned, frictionally constrained fibers, J. Mech. Phys. Solids 37 (1989) 93–109.
[4] P.F. Becher, Microstructural design of toughened ceramics, J. Am. Ceram. Soc. 74 (1991) 255–269.
[5] K.T. Faber, A.G. Evans, Crack deflection processes: I. Theory, Acta. Metall. 31 (4) (1983) 565–576.
[6] J.Y. Kim, J.W. Kim, J.G. Lee, K.S. Cho, Effect of annealing on mechanical properties of self-reinforced alpha-silicon carbide, J. Mater. Sci. 34 (1999) 2325–2330.
[7] Y.W. Kim, M. Mitomo, H. Emoto, J.G. Lee, Effect of Initial α-phase content on microstructure and mechanical properties of sintered silicon carbide, J. Am. Ceram. Soc. 81 (12) (1998) 3136–3140.
[8] C.H. McMurty, W.D. Boecker, S.G. Seshadri, J.S. Zanghi, J. Garnier, Microstructure and materials properties of SiC–TiB_2 particulate composites, J. Am. Ceram. Soc. Bull. 66 (2) (1987) 325–329.

[9] K.S. Cho, Y.W. Kim, H.J. Choi, J.G. Lee, SiC–TiC and SiC–TiB_2 composites densified by liquid phase sintering, J. Mater. Sci. 31 (1996) 6223–6228.
[10] A.K. Khaund, V.D. Krstic, P.S. Nicholson, Influence of elastic and thermal mismatch on the local crack-driving force in brittle composites, J. Mater. Sci. 12 (1977) 2269–2273.
[11] J.D. Yoon, S.G. Kang, Strengthening and toughening behavior of SiC with addition of TiB_2, J. Mater. Sci. Lett. 14 (1995) 1065–1067.
[12] K.S. Cho, H.J. Choi, J.G. Lee, In situ enhancement of toughness of SiC–TiB_2 composites, J. Mater. Sci. 33 (1998) 211–214.
[13] F. De Maestral, F. Thevenot, Ceramic composites: TiB_2–TiC–SiC: Part I. Properties and microstructures in the ternary system, J. Mater. Sci. 26 (1991) 5547–5560.
[14] T. Tani, S. Wada, SiC matrix composites containing transition metal boride particulates internally synthesized by carbothermal reaction, J. Mater. Sci. 26 (1991) 3526–3532.
[15] M.A. Mulla, V.D. Krstic, Low-temperature pressureless sintering of β-silicon carbide with aluminum oxide and yttrium oxide additions, Ceram. Bull. 70 (3) (1991) 439–443.
[16] G.R. Anstis, P. Chantikul, B.R. Lawn, D.B. Marshall, A critical evaluation of indentation techniques for measuring fracture toughness: I. Direct crack measurements, J. Am. Ceram. Soc. 64 (1981) 533–538.
[17] D. Munz, R.T. Bubsey, J.L. Shannon, Fracture toughness determination of Al_2O_3 using four-point-bend specimens with straight-through and chevron notches, J. Am. Ceram. Soc. 63 (1980) 300–305.
[18] J.S. Abell, I.R. Harris, B. Cockayne, B. Lent, An investigation of phase stability in the Y_2O_3–Al_2O_3 system, J. Mater. Sci. 9 (1974) 527–537.